Effect of reduction temperature on the electrochemical properties of a Ni/YSZ anode-supported solid oxide fuel cell

Ting Shuai Li, Wei Guo Wang, He Miao, Tao Chen, Cheng Xu *

Division of Fuel Cell and Energy Technology, Ningbo Institute of Material Technology & Engineering, Chinese Academy of Sciences, 519 Zhuangshi Road, Ningbo 315201, China

A R T I C L E   I N F O

A B S T R A C T

The influence of reduction temperature on the anodic microstructure and electrochemical properties of a typical nickel/yttria-stabilized zirconia anode-supported solid oxide fuel cell (SOFC) has been investigated in a range of temperatures from 550 °C to 750 °C. The cell reduced at 650 °C yields the largest power output (P_{max} = 0.56 W cm^{-2} at 850 °C) and the lowest area specific resistance (ASR = 0.5 Ω cm^2 at 850 °C). Electrochemical impedance spectrum (EIS) analysis shows that the cell reduced at 650 °C exhibits the lowest polarization resistance (R_p) of 0.72 Ω cm^2, which is in good agreement with the results from *i–V* curves. Nickel agglomeration is observed in the anode for the cells reduced at 550 °C and 750 °C while a homogeneous anodic microstructure is inspected for the cell reduced at 650 °C, suggesting reduction process has a vital effect on the anodic microstructure of the cell before aging.

1. Introduction

The anode-supported solid oxide fuel cell (SOFC) has attracted much attention as an effective clean energy converter for its potential to provide high power density [1]. The most commonly used anode material for the SOFC cell is a double phase of nickel and yttria-stabilized zirconia (Ni/YSZ) [2], which has been widely investigated in terms of material fabrication [3,4], chemical stability [5,6] and characterization [7,8]. Desired anodic microstructure is an anode composed of NiO and YSZ particles with similar sizes [9]. The Ni/YSZ volume ratio has also a significant influence on cell performance including power output, IR resistance and polarization resistance [10]. Wilson and Barnett [11] reported that the highest triple phase boundary density was at a Ni:YSZ volume ratio of ~0.5, which enhanced the electrochemical reactions at the anode greatly. The maximum power density of SOFC cells was also shown to be greatly dependent on the anodic microstructure [12–14]. Kim et al. [13] showed that the anode layer with a highly reactive and uniform electrode microstructure reduced the polarization resistance of the SOFC single cell from 1.07 Ω cm^2 to 0.48 Ω cm^2 at 800 °C.

Besides the powder size and the volume ratio of NiO to YSZ, operation condition is also found to affect cell performance for both a short period and a long duration [15–17]. This may be because the anode microstructure develops during cell operation and this development is directly associated with cell testing conditions.

Haanappel et al. [15] showed that electrode activation was much faster for the cell reduced at 900 °C than the cell reduced at 800 °C and the electrode activation was incomplete unless the tested cell was at least heated to and reduced at 900 °C. This implies that a reduction temperature interval of 100 °C could result in different cell performances. However, the effect of reduction procedure on the long-term performance of the cell is limited since the total degradation over 1000 h is only ~1% [16] and the reduction is realized by a short-term current load for less than 10 h at the beginning of aging. The degradation mechanism for anode has been considered to be mainly related to nickel agglomeration [17] and thus reduction in electrochemical reaction sites would definitely cause cell performance degradation.

In summary, the initial anodic microstructure is important to the cell performance, especially over a short period, and the reduction procedure is crucial to the initial anodic microstructure. Therefore, it is necessary to define the reduction process in order to achieve optimized initial microstructure of the cell. The present investigation is thus initiated to evaluate the effect of reduction temperature ranging from 550 °C to 750 °C on anode microstructure and cell performance. Impedance spectra are monitored during reduction process and anodic microstructure is closely inspected to give an insight on reducing course.

2. Experimental

Experiments were conducted using a typical anode-supported SOFC single cell manufactured by Division of Fuel Cell and Energy Technology in Ningbo Institute of Material Technology & Engineering, Chinese Academy of Sciences. The cell consisted of a Ni/8YSZ anode substrate of 400 μm thick, a functional layer of 10 μm thick, an 8YSZ electrolyte layer of 10 μm thick and a double layer of strontium-doped

* Corresponding author. Tel.: +86 574 87915139.
E-mail address: xucheng@nimte.ac.cn (C. Xu).

lanthanum manganite perovskite (LSM) cathode. All the tests were carried out using 3 identical samples cut from a single cell with dimensions of 12 cm × 12 cm. All samples had dimensions of 5 cm × 5.8 cm with an active area of 4 cm × 4 cm.

All samples were tested in an alumina testing house with platinum patch and nickel foil as current collectors at cathode and anode sides, respectively. For better gas distribution, nickel mesh and LSM plate were also utilized at anode and cathode sides, respectively. Ceramic glass mainly consisting of silicon dioxide was used as sealant with an external weight of 5.5 kg for good sealing. The samples were then heated in an electric furnace at a heating rate of 1 °C min⁻¹ to 850 °C and retained at 850 °C for more than 3 h to intenerate the sealant. The reduction was carried out subsequently at temperatures of 550 °C, 650 °C and 750 °C up to 5 h using pure hydrogen with a flow rate of 300 Nml min⁻¹ as anode fuel and air as cathode gas with a flow rate of 500 Nml min⁻¹.

After reduction for 5 h, air and pure hydrogen were introduced into the cathode and the anode with a flow rate of 2000 Nml min⁻¹ and 800 Nml min⁻¹, respectively. The electrical properties of the cell were recorded at different operation temperatures ranging from 650 °C to 850 °C. Electrochemical impedance spectrum (EIS) measurements were taken at open circuit voltage (OCV) by four-electrode configuration using an Electrochemical Workstation (IM6ex, ZAHNER) with frequencies ranging from 0.1 Hz to 2 MHz. To determine the reduction degree of the sample using different reduction courses, the EIS measurements were taken during the reduction process at least every 30 min.

Microstructural observation was conducted using a HITACHI S4800 scanning electron microscope (SEM) and the distribution of Ni element in the anode of the as-tested cell was inspected using an energy dispersive spectroscopy (EDS).

3. Results and discussion

Fig. 1a shows the EIS results for the cell reduced at 550 °C for different time periods. The impedance of the cell decreases dramatically with the increasing reduction time in the first couple of hours and then declines slowly until stabilization after 4 h. Fig. 1b displays the variation of OCV of the cell reduced at 550 °C with the reduction time where the OCV achieves saturation after reduction for 4 h. Therefore, a complete reduction of the anode is obtained after reduction for 5 h at 550 °C. Since the reduction is a thermal-activated process, the cell is completely reduced after 5 h at temperatures above 550 °C.

Fig. 2 shows the performance of single cells reduced at temperatures of 550 °C, 650 °C and 750 °C for 5 h and then tested at 700 °C, 750 °C, 800 °C and 850 °C, respectively, where the curves with solid points denote i–V curves of the cells while open points denote the variation of output power with current density. According to the discussion based on the results in Fig. 1, all the cells subjected to electrochemical testing are fully reduced. Among these cells, the single cell reduced at 650 °C yields the highest power output under all operation temperatures and achieves a maximum power density (P_{max}) of 0.5 W cm⁻² at 850 °C whereas the P_{max} for the single cells reduced at 550 °C and 750 °C are 0.45 W cm⁻² and 0.42 W cm⁻², respectively.

As an important performance parameter, the area specific resistance (ASR) is calculated using Eq. (1):

$$\text{ASR} = \frac{\text{OCV} - 0.7}{I_{0.7}} \tag{1}$$

where OCV is the open circuit voltage and $I_{0.7}$ is the discharging current density at a voltage of 0.7 V. The results are summarized in Table 1. It is apparent that the cell reduced at 650 °C has the lowest ASR over all operation temperatures. This is consistent with the
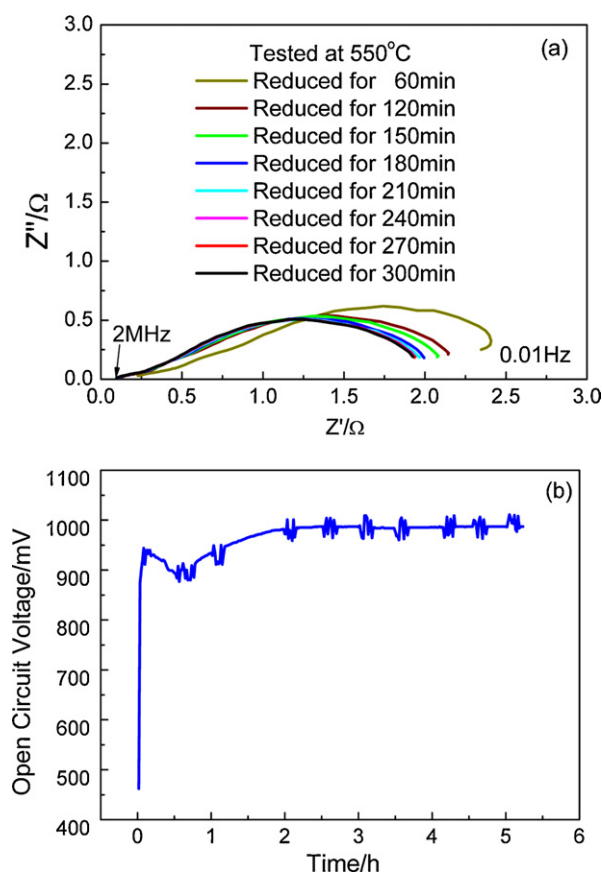

Fig. 1. Electrochemical impedance spectra recorded during reduction process at 550 °C.

results shown in Fig. 2 where the cell reduced at 650 °C exhibits the highest performance.

It is known that the resistance of the cell is greatly dependent on operation temperature. This temperature dependence can be described using Arrhenius empirical equation:

$$\ln \sigma = \ln A - \frac{E_a}{RT} \tag{2}$$

where σ is the conductivity of the single cell equivalent to the reciprocal of ASR, E_a is the activation energy in eV, R is the gas constant, T is the absolute temperature of operation and A is a constant independent of temperature. The conductivity of the cell is thus plotted logarithmically against $1/T$ as shown in Fig. 3 to calculate E_a and the results are listed in Table 1. It is apparent the single cell reduced at 650 °C obtains the lowest E_a of 0.52 eV by comparison with the other two cells reduced at different temperatures.

Electrochemical impedance spectra (EIS) of the single cells were measured and the results are shown in Fig. 4. The cells reduced at different temperatures exhibit similar series resistance (denoted as R_s) whereas dramatic deviation in polarization resistance (denoted

Table 1
The electrochemical properties (including P_{max}, ASR, R_p and R_s) of SOFC reduced at various temperatures under the operation temperatures (650–850 °C).

	Reduced at 550 °C				Reduced at 650 °C				Reduced at 750 °C			
	700 °C	750 °C	800 °C	850 °C	700 °C	750 °C	800 °C	850 °C	700 °C	750 °C	800 °C	850 °C
P_{max}/W cm⁻²	0.19	0.30	0.41	0.50	0.25	0.39	0.50	0.56	0.19	0.30	0.41	0.47
ASR/Ω cm²	1.67	1.16	0.78	0.61	1.32	0.82	0.62	0.55	2.08	1.37	0.90	0.71
E_a/eV		0.64				0.52				0.78		
R_s/Ω cm²	0.36	0.29	0.17	0.17	0.29	0.2	0.19	0.17	0.24	0.27	0.14	0.14
R_p/Ω cm²	3.10	2.24	1.63	0.84	1.69	1.20	0.95	0.65	3.00	2.25	1.66	1.66

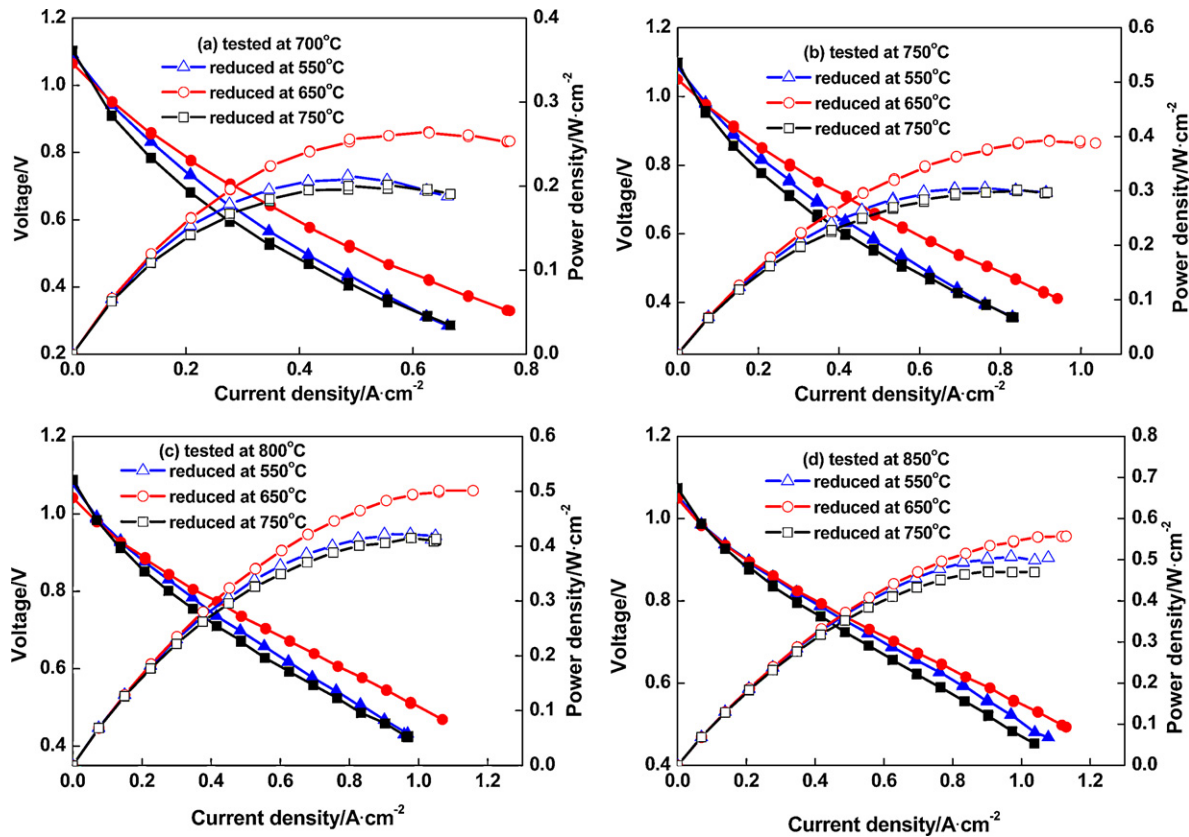**Fig. 2.** i–V curves for single cells reduced at different temperatures from 550 °C to 750 °C under operation temperatures of: 700 °C (a); 750 °C (b); 800 °C (c); 850 °C (d).

as R_p) is observed at all operating temperatures (550–750 °C) although the R_p for all cells decreases with the increasing temperature. Among the cells reduced at different temperatures, the cell reduced at 650 °C produces the smallest R_p, which is recorded at 850 °C.

Reduction time has also a significant effect on the performance of the single cell. As shown in Fig. 1 for the cell reduced at 550 °C, reduction time effect is significant in the first couple of hours. The EIS for the cell reduced at 650 °C is thus recorded at different time periods within 1 h as shown in Fig. 5 to give a closer inspection of the reduction time effect. Apparently, the polarization resistance decreases continuously with increasing reduction time while series resistance (R_s) shows no variation as time increases. Since electrolyte resistance and interfacial resistance at

electrodes/electrolyte are largely reflected by R_s [18], it is suggested that the reduction process has no influence on the electrolyte and electrodes/electrolyte interfaces. The reduction produces Ni by hydrogen atoms rupturing Ni–O bonds. These nickel atoms may diffuse across the surface of anode support to be away from the center of reduction and thereby nucleate into metallic clusters [19], leading to acceleration in charge transfer. Moreover, anode porosity increases as NiO is chemically converted to Ni because of molar volume variation of metallic nickel and nickel oxide [20]. The porosity increase in the anode is in favor of mass transfer and gas conversion, resulting in cell polarization resistance decrease in the low frequency range [21]. The polarization resistance thus decreases with increasing reduction time.

The reduction mechanism of the cell is further inspected by plotting the difference of EIS for each single cell reduced for 10 and 30 min, denoted by ΔZ, against logarithmic frequency, denoted as $\log f$, as shown in Fig. 6. The ΔZ can be thus identified by Eq. (3) [21]

$$\Delta Z = \frac{\partial Z^{time2}}{\log f} - \frac{\partial Z^{time1}}{\log f} \tag{3}$$

where Z^{time} denotes real part of impedance spectra gained at a certain reduction time and f is the frequency domain. It is apparent the ΔZ for each single cell displays a peak value at low frequency range (below 2 Hz) which is reported to involve gas diffusion and gas conversion processes at anode side [22]. In the reduction course, there is only one relevant chemical reaction (Eq. (4)) where

$$NiO + H_2 = Ni + H_2O \tag{4}$$

Thus the deviation of the impedance spectra may reflect the extent of NiO being converted to Ni. With the increase of reduction temperature, the deviation peak shifts to higher frequencies, indicating higher reduction rate for NiO at higher reduction temperatures. At the same time, it is established that a proper reduction
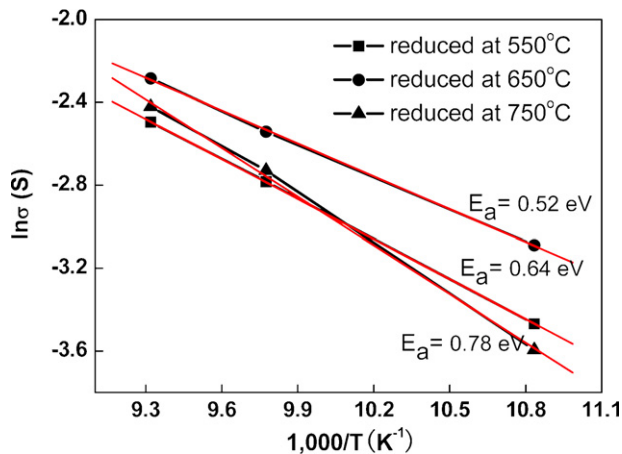

Fig. 3. $\ln\sigma$ versus $1/T$ for the single cell reduced at different temperatures.
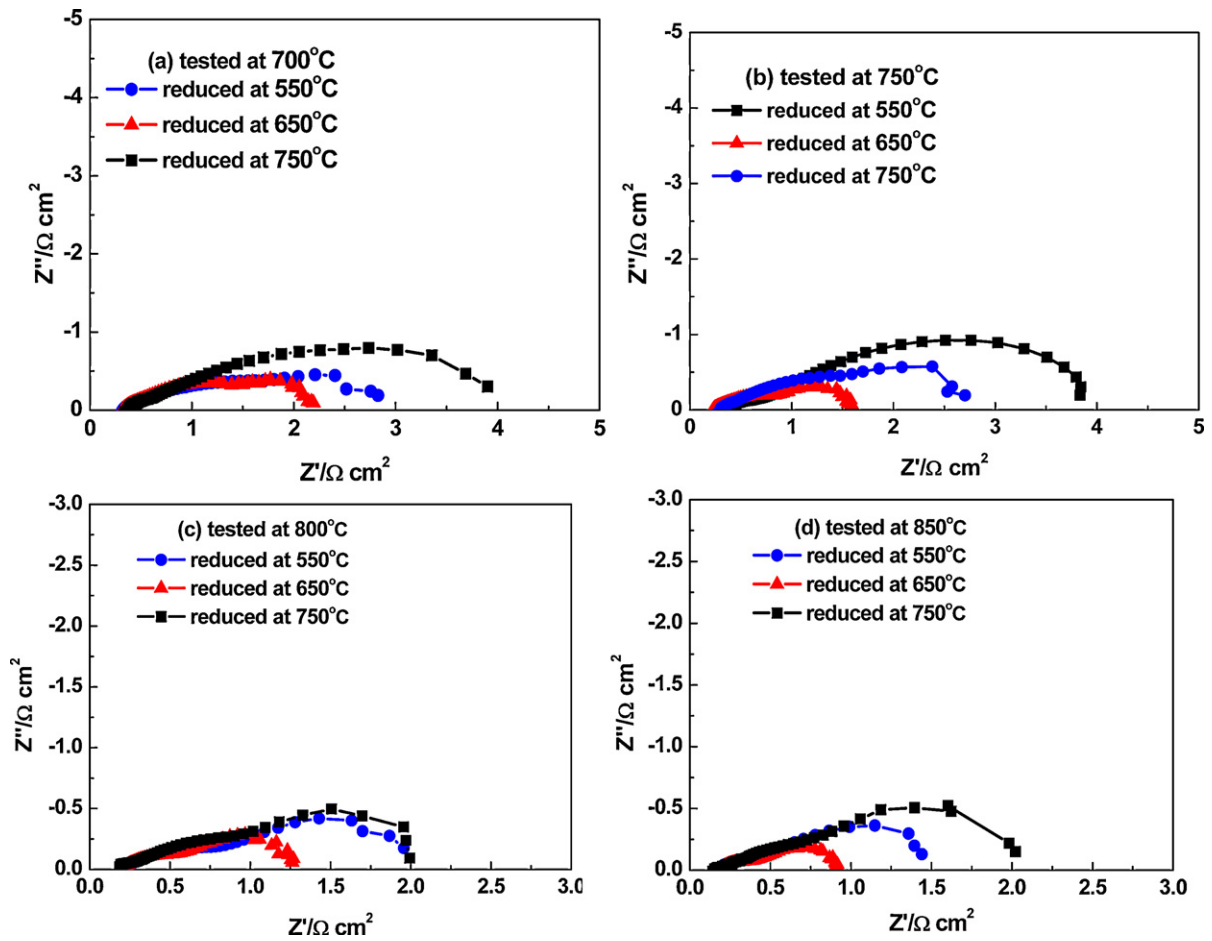
Fig. 4. Electrochemical impedance spectra (EIS) for the single cells reduced at different temperatures and then tested at: 700 °C (a); 750 °C (b); 800 °C (c); 850 °C (d).

rate of NiO is important to obtain a homogeneous microstructure [23]. The cell reduced at 650 °C exhibits a summit frequency of 0.8 at the maximum conversion of NiO to Ni, which may be the closest to the proper conversion rate among all investigated reduction temperatures. It is thus concluded that 650 °C is a proper reduction temperature for the SOFC single cell based on Ni/YSZ anode in our study.

Fig. 7 shows representative SEM pictures for the anodes of the cells reduced at different temperatures for 5 h. It is clear that the surface morphologies of SOFC anodes reduced at different temper-

Fig. 5. Electrochemical impedance spectra recorded in reduction process at 650 °C.

atures are different in nickel distribution. Nickel agglomerations of significant sizes can be detected easily in the cell reduced at 550 °C and 750 °C while a much more homogeneous microstructure is observed in the cell reduced at 650 °C. Specifically, the nickel agglomerations having a size of ten microns in diameter can be observed in the active layer of the Ni-YSZ anode for the single cell reduced at 550 °C while the cell reduced at 750 °C exhibits nickel particles with diameters of several microns dispersed in both anodic substrate area and active region of the Ni-YSZ anode. This may explain the good performance of the cell reduced at 650 °C.

Generally speaking, the SOFC process involves dissociative adsorption of H_2 and transport to triple phase boundaries (TPBs), charge transfer and gas diffusion and conversion [10] and these processes can be interpreted quantitatively as activation resistance, bulk resistance and concentration resistance, respectively. For the cells reduced at different temperatures, bulk resistance and concentration resistance may be the dominating factors. Bulk resistance and concentration resistance are majorly determined by the anodic microstructure because there is no evident deviation for electrochemical properties in relatively low current density dominated by activation process. But in high current density domain, much different power output is recorded.

It is also observed that the size of nickel particles in Ni/YSZ cermet tends to increase during operation resulting in the decrease (loss) of specific surface area and conductivity of the anode and eventually deterioration of the cell performance. Therefore, nickel agglomeration is detrimental to cell operation at an optimal performance. According to the impedance spectra results shown in Fig. 6, NiO can be quickly converted to Ni within 1 h reduction. In the meanwhile, reassembly and successive reduction of nickel
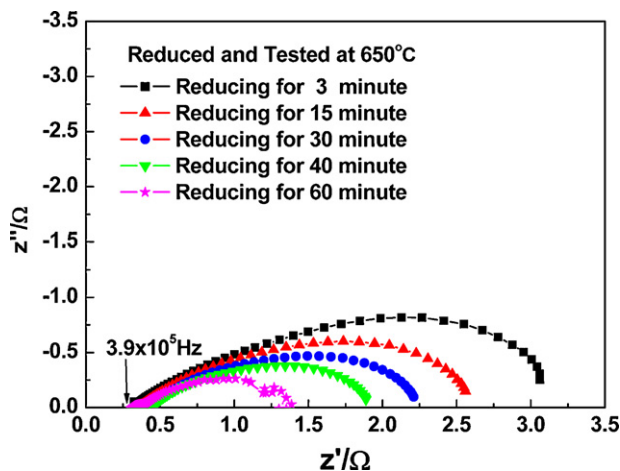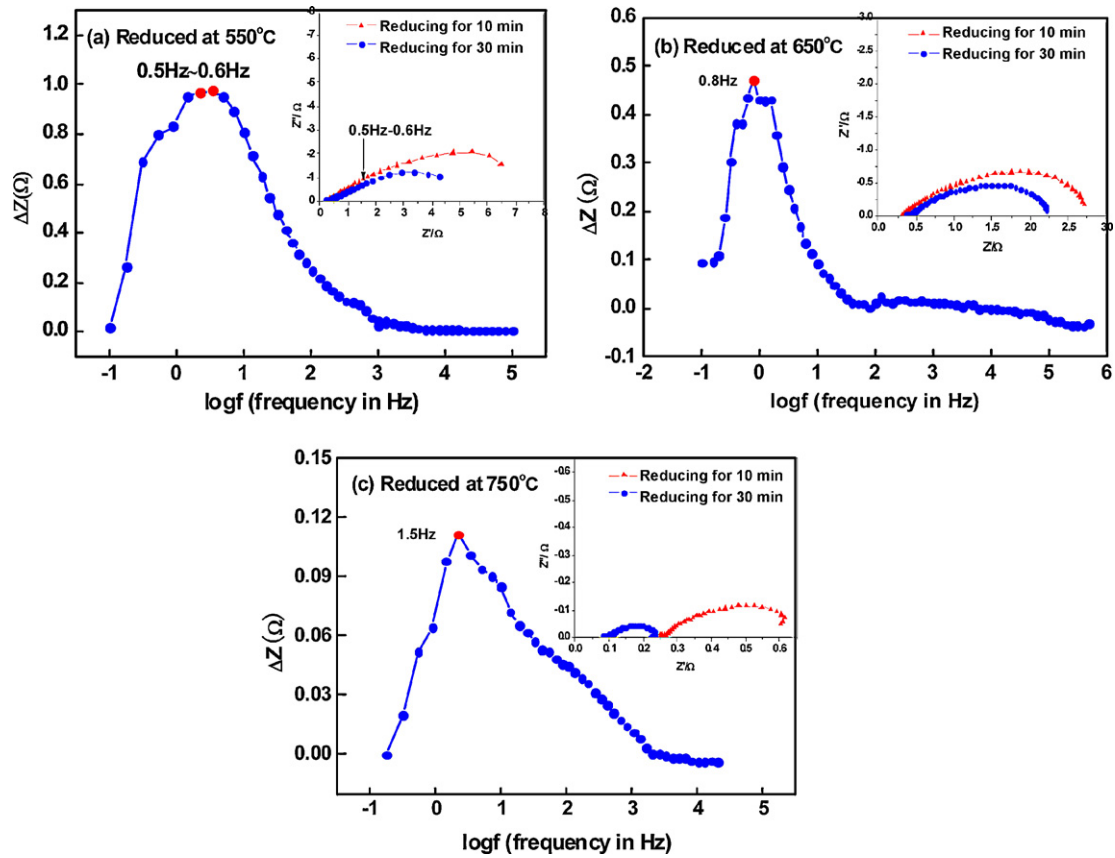
Fig. 6. The ΔZ versus logarithmic frequency for cell reduced at temperatures: 550 °C (a); 650 °C (b); 750 °C (c).
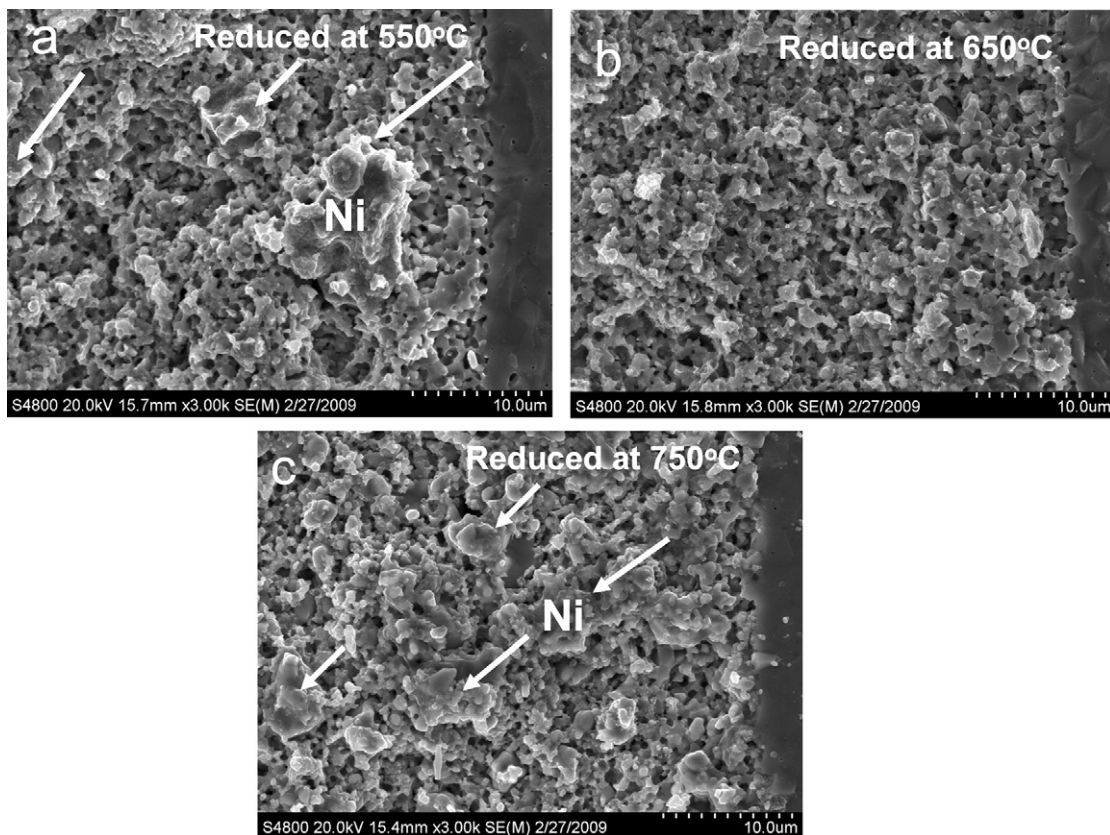

Fig. 7. Representative SEM images of SOFC anode reduced at temperatures: 550 °C (a); 650 °C (b); 750 °C (c).

particles occur. The conducting properties of nickel in anode are pertinent to microstructure and the specific area of YSZ. High temperature sintering and reduction process are thus crucial to anodic microstructure. With more NiO being reduced to Ni, reduction in particle size will lead less contact among particles and less conductivity. Therefore, the nickel agglomeration observed in cells reduced at 550 °C and 750 °C can be attributed to an improper reducing rate in our work.

4. Conclusions

In this paper, the effects of reduction temperatures (550–750 °C) on the electrochemical properties and microstructure of the anode-supported SOFC single cell were investigated in detail. The results indicated that the single cell reduced at 650 °C obtained the best electrochemical properties, achieving a P_{max} of 0.5 W cm^{-2} and an ASR of 0.5 Ω cm^2 at 850 °C. This may be because the single cell reduced at 650 °C has the most homogeneous microstructure. Therefore, 650 °C may be the optimum reduction temperature for Ni/YSZ anode-supported SOFC cell.

Acknowledgements

References

[1] EG&G Technical Services, Inc., Fuel Cell Handbook, vol. 7, seventh edition, 2004, solid oxide fuel cell.
[2] T. Fukui, S. Ohara, K. Mukai, Electrochem. Solid-State Lett. 1 (3) (1998) 120–122.
[3] L. Jia, Z. Lu, J. Miao, Z. Liu, G. Li, W. Su, J. Alloys Compd. 414 (2006) 152–157.
[4] H.S. Hong, U.S. Chae, S.T. Choo, J. Alloys Compd. 449 (2008) 331–334.
[5] S. Lee, K.H. Kang, H.S. Hong, Y. Yun, J.H. Ahn, J. Alloys Compd. 488 (2009) L1–L5.
[6] J.J. Choi, J. Ryu, B.D. Hahn, W.H. Yoon, B.K. Lee, J.H. Choi, D.S. Park, J. Alloys Compd. (2009), doi:10.1016/j.jallcom.2009.11.146.
[7] K. Thydén, Y.L. Liu, J.B. Bilde-Sørensen, Solid State Ionics 178 (2008) 1984–1989.
[8] H. Xiao, T.L. Reitz, M.A. Rottmayer, J. Power Sources 183 (2008) 49–54.
[9] C.H. Lee, C.H. Lee, H.Y. Lee, S.M. Oh, Solid State Ionics 98 (1997) 39–48.
[10] H. Koide, Y. Someya, T. Yoshida, T. Maruyama, Solid State Ionics 132 (2000) 253–260.
[11] J.R. Wilson, S.A. Barnett, Electrochem. Solid-State Lett. 11 (10) (2008) B181–B185.
[12] C.X. Li, C.J. Li, L.J. Guo, Int. J. Hydrogen Energy 33 (2008) 3945–3951.
[13] S. Kim, J. Lee, H. Moon, S. Hyun, J. Moon, J. Kim, H. Lee, J. Power Sources 169 (2007) 265–270.
[14] N.F.P. Ribeiro, M.M.V.M. Souza, O.R.M. Neto, S.M.R. Vasconcelos, M. Schmal, Appl. Catal. A: Gen. 353 (2009) 305–309.
[15] V.A.C. Haanappel, A. Mai, J. Mertens, Solid State Ionics 177 (2006) 2033–2037.
[16] V.A.C. Haanappel, B. Röwekamp, C. Tropartz, H. Wesemeyer, M.J. Smith, L.G.J. (Bert) de Haart, Oral Presentation, Session B09, Testing, Thursday, July 3, 2008.
[17] H. Tu, U. Stimming, J. Power Sources 127 (2004) 284–293.
[18] W.G. Wang, M. Mogensen, Solid State Ionics 176 (2005) 457–462.
[19] J.T. Richardson, R.M. Scates, M.V. Twigg, Appl. Catal. A: Gen. 267 (2004) 35–46.
[20] A. Faes, A. Nakajo, A.H. Wyserb, D. Duboisb, A. Brissec, S. Modenad, J. Van herle, J. Power Sources 193 (2009) 55–64.
[21] R. Barfod, M. Mogensen, T. Klemensø, A. Hagen, Y. Liu, P.V. Hendriksen, J. Electrochem. Soc. 154 (4) (2007) B371–B378.
[22] R. Barfod, A. Hagen, S. Ramousse, P.V. Hendriksen, M. Mogensen, Fuel Cells 6 (2) (2006) 141–145.
[23] Y. Zhang, B. Liu, B. Tu, Y. Dong, M. Cheng, Solid State Ionics 176 (2005) 2193–2199.